Using shaped ultrafast laser pulses to detect enzyme binding

Chien-hung Tseng,[1] **Thomas C. Weinacht,**[1] **Anna E. Rhoades,**[2] **Matthew Murray,**[3] **and Brett J. Pearson**[3,*]

[1]*Department of Physics and Astronomy, Stony Brook University, Stony Brook, NY, 11794-3800 USA*
[2]*Department of Molecular Biophysics and Biochemistry, Yale University, New Haven, CT, 06520-8114 USA*
[3]*Department of Physics and Astronomy, Dickinson College, Carlisle, PA 17013-2896 USA*
[*]*pearsonb@dickinson.edu*

Abstract: We use multiphoton quantum-control spectroscopy to discriminate between unbound and enzyme-bound NADH (reduced nicotinamide adenine dinucleotide) molecules in solution. Shaped ultrafast laser pulses are used to illuminate both forms of NADH, and the ratio of the fluorescence from the bound and unbound molecules for different pulse shapes allows us to measure binding without spectrally resolving the emitted fluorescence or relying on the absolute fluorescence yield. This permits determination of enzyme binding in situations where spectrally resolved measurements and absolute fluorescence yields are difficult to obtain, and makes the approach ideal for multiphoton microscopy with molecular discrimination.

© 2011 Optical Society of America

OCIS codes: (320.5540) Ultrafast pulse shaping; (320.7150) Ultrafast spectroscopy; (170.6280) Spectroscopy, fluorescence and luminescence.

References and links

1. P. Brumer and M. Shapiro, "Control of unimolecular reactions using coherent light," Chem. Phys. Lett. **126**, 541–546 (1986).
2. D. J. Tannor, R. Kosloff, and S. A. Rice, "Control pulse sequence induced control of selectivity of reactions: Exact quantum mechanical calculations," J. Chem. Phys. **85**, 5805–5820 (1986).
3. H. Rabitz, R. de Vivie-Riedle, M. Motzkus, and K. Kompa, "Whither the future of controlling quantum phenomena?" Science **288**, 824–828 (2000).
4. T. Brixner and G. Gerber, "Quantum control of gas-phase and liquid-phase femtochemistry," ChemPhysChem **4**, 418–438 (2003).
5. M. A. Dugan, J. X. Tull, and W. S. Warren, "High resolution acousto-optic shaping of unamplified and amplified femtosecond laser pulses," J. Opt. Soc. Am. B **14**, 2348–2358 (1997).
6. A. M. Weiner, "Femtosecond pulse shaping using spatial light modulators," Rev. Sci. Inst. **71**, 1929–1960 (2000).
7. R. S. Judson and H. Rabitz, "Teaching lasers to control molecules," Phys. Rev. Lett. **68**, 1500–1503 (1992).
8. W. Denk, J. Strickler, and W. W. Webb, "Two-photon laser scanning fluorescence microscopy," Science **248**, 73–76 (1990).
9. W. R. Zipfel, R. M. Williams, and W. W. Webb, "Nonlinear magic: multiphoton microscopy in the biosciences," Nature Biotech. **21**, 1369–1377 (2003).
10. J.-X. Cheng and X. S. Xie, "Coherent anti-Stokes Raman scattering microscopy: Instrumentation, theory, and applications," J. Phys. Chem. B **108**, 827–840 (2004).
11. N. Dudovich, D. Oron, and Y. Silberberg, "Single-pulse coherently controlled nonlinear Raman spectroscopy and microscopy," Nature **418**, 512–514 (2002).
12. B. von Vacano and M. Motzkus, "Molecular discrimination of a mixture with single-beam Raman control," J. Chem. Phys. **127**, 144514 (2007).
13. X. G. Xu, S. O. Konorov, J. W. Hepburn, and V. Milner, "Noise autocorrelation spectroscopy with coherent Raman scattering," Nature Phys. **4**, 125–129 (2008).

#155285 - $15.00 USD Received 26 Sep 2011; revised 13 Oct 2011; accepted 15 Oct 2011; published 16 Nov 2011
(C) 2011 OSA

14. B. von Vacano and M. Motzkus, "Time-resolving molecular vibration for microanalytics: single laser beam nonlinear Raman spectroscopy in simulation and experiment," Phys. Chem. Chem. Phys. **10**, 681–691 (2008).
15. A. C. W. van Rhijn, S. Postma, J. P. Korterik, J. L. Herek, and H. L. Offerhaus, "Chemically selective imaging by spectral phase shaping for broadband CARS around 3000 cm^{-1}," J. Opt. Soc. Am. B **26**, 559–563 (2009).
16. J. Rehbinder, C. Pohling, T. Buckup, and M. Motzkus, "Multiplex coherent anti-Stokes Raman microspectroscopy with tailored Stokes spectrum," Opt. Lett. **35**, 3721–3723 (2010).
17. W. Wohlleben, T. Buckup, J. L. Herek, and M. Motzkus, "Coherent control for spectroscopy and manipulation of biological dynamics," ChemPhysChem **6**, 850–857 (2005).
18. K. A. Walowicz, I. Pastirk, V. V. Lozovoy, and M. Dantus, "Multiphoton intrapulse interference. 1. Control of multiphoton processes in condensed phases," J. Phys. Chem. A **106**, 9369–9373 (2002).
19. J. M. D. Cruz, V. V. Lozovoy, and M. Dantus, "Coherent control improves biomedical imaging with ultrashort shaped pulses," J. Photochem. Photobio. A **180**, 307 – 313 (2006).
20. J. P. Ogilvie, D. Débarre, X. Solinas, J.-L. Martin, E. Beaurepaire, and M. Joffre, "Use of coherent control for selective two-photon fluorescence microscopy in live organisms," Opt. Express **14**, 759–766 (2006).
21. R. S. Pillai, C. Boudoux, G. Labroille, N. Olivier, I. Veilleux, E. Farge, M. Joffre, and E. Beaurepaire, "Multiplexed two-photon microscopy of dynamic biological samples with shaped broadband pulses," Opt. Express **17**, 12741–12752 (2009).
22. I. Pastirk, J. M. D. Cruz, K. A. Walowicz, V. V. Lozovoy, and M. Dantus, "Selective two-photon microscopy with shaped femtosecond pulses," Opt. Express **11**, 1695–1701 (2003).
23. T. Brixner, N. H. Damrauer, P. Niklaus, and G. Gerber, "Photoselective adaptive femtosecond quantum control in the liquid phase," Nature **414**, 57–60 (2001).
24. M. Roth, L. Guyon, J. Roslund, V. Boutou, F. Courvoisier, J.-P. Wolf, and H. Rabitz, "Quantum control of tightly competitive product channels," Phys. Rev. Lett. **102**, 253001 (2009).
25. T. Weinacht, "Distinguishing between molecules that look the same," Physics **2**, 51 (2009).
26. S. D. Clow, U. C. Hölscher, and T. C. Weinacht, "Achieving "perfect" molecular discrimination via coherent control and stimulated emission," New J. Phys. **11**, 115007 (2009).
27. K. A. Kasischke, H. D. Vishwasrao, P. J. Fisher, W. R. Zipfel, and W. W. Webb, "Neural activity triggers neuronal oxidative metabolism followed by astrocytic glycolysis," Science **305**, 99–103 (2004).
28. H. D. Vishwasrao, A. A. Heikal, K. A. Kasischke, and W. W. Webb, "Conformational dependence of intracellular NADH on metabolic state revealed by associated fluorescence anisotropy," J. Bio. Chem. **280**, 25119–25126 (2005).
29. H. D. Vishwasrao, "Quantitative two-photon redox fluorescence microscopy of neurometabolic dynamics," Ph.D. thesis, Cornell University (2005).
30. D. Meshulach and Y. Silberberg, "Coherent quantum control of multiphoton transitions by shaped ultrashort optical pulses," Phys. Rev. A **60**, 1287–1292 (1999).
31. A. Gandman, L. Chuntonov, L. Rybak, and Z. Amitay, "Coherent phase control of resonance-mediated $(2+1)$ three-photon absorption," Phys. Rev. A **75**, 031401 (2007).
32. C. Trallero-Herrero and T. C. Weinacht, "Transition from weak- to strong-field coherent control," Phys. Rev. A **75**, 063401 (2007).
33. R. Trebino, K. W. DeLong, D. N. Fittinghoff, J. N. Sweetser, M. A. Krumbugel, B. A. Richman, and D. J. Kane, "Measuring ultrashort laser pulses in the time-frequency domain using frequency-resolved optical gating," Rev. Sci. Inst. **68**, 3277–3295 (1997).
34. Y. Silberberg, "Quantum coherent control for nonlinear spectroscopy and microscopy," Ann. Rev. Phys. Chem. **60**, 277–292 (2009).
35. J. J. Holbrook and R. G. Wolfe, "Malate dehydrogenase. X. fluorescence microtitration studies of d-malate, hydroxymalonate, nicotinamide dinucleotide, and dihydronicotinamide-adenine dinucleotide binding by mitochondrial and supernatant porcine heart enzymes," Biochemistry **11**, 2499 (1972).
36. Developmental Resource for Biophysical Imaging Opto-Electronics (DRBIO) at Cornell University, "Two-photon action cross sections," http://www.drbio.cornell.edu/cross_sections.html.

1. Introduction

Over the past two decades, the field of coherent control has developed with the goal of preparing molecules in specific quantum states [1–4]. Just as light diffracting from two slits can interfere to produce dark and bright bands on a distant screen (such as in a "Young's double-slit experiment"), interference between multiple quantum paths to a final state in the molecular excitation process can result in selective excitation of one molecule or molecular state over another. Coherent control over quantum systems is typically achieved by varying the phase of the laser light used for excitation, either by changing the phase between two laser beams or shaping broadband light from an ultrafast laser pulse. The shaping is accomplished with an ultrafast pulse

#155285 - $15.00 USD Received 26 Sep 2011; revised 13 Oct 2011; accepted 15 Oct 2011; published 16 Nov 2011
(C) 2011 OSA

shaper, in which frequency components comprising the pulse are each mapped to a unique point in space using a diffraction grating and focusing optic. A programmable mask (such as a liquid crystal display or acousto-optic modulator) is used to adjust the phase and amplitude of each spatially-resolved frequency component before they are reassembled using a second optic and grating [5, 6]. Because the electric field in time can be expressed in terms of its frequency components, shaping the pulse in the frequency domain allows for the creation of an arbitrary pulse in time within the bandwidth limits of the laser and pulse shaper. With a programmable mask, one can switch between pulse shapes rapidly, enabling fast pulse shape scans, as well as closed-loop control experiments [7], where an iterative approach is used to discover pulse shapes well-suited to preparing a desired quantum state of the system.

Parallel advances in cellular imaging techniques have revolutionized our ability to study complex biological and chemical processes. In particular, the development of multiphoton imaging [8–10] has greatly expanded applications of microscopy in biochemical systems, while imaging with techniques such as coherent anti-Stokes Raman (CARS) microscopy [11–16] has allowed for chemical selectivity in microscopic samples. CARS microscopy with shaped laser pulses is one particular example of "quantum-control spectroscopy," in which a molecular response is measured as a function of pulse shape, rather than the frequency of a single excitation source [17]. While both fields have advanced greatly, applications of coherent control toward cellular imaging have come only recently, despite the fact that pulse shaping has several advantages for imaging living cells, including the inherent compensation of pulse broadening (chirp) that reduces image quality and suppression of three-photon absorption, a major cause of photodamage in multiphoton imaging [18, 19]. The few papers that have been published provide proof-of-principle, showing, for example, that coherent control can discriminate between endogenous cell fluorescence and green fluorescent protein (GFP) in drosophila embryos [20, 21], or selectively excite GFP in a pH-dependent manner [19]. However additional control experiments suggest that coherent control has the potential to become an even more powerful component of multiphoton imaging. For example, intramolecular selectivity has been demonstrated [18, 22, 23], as well as selectivity between separate molecules with almost identical single-photon excitation spectra [23–26].

In this paper we use quantum-control spectroscopy to discriminate between unbound and enzyme-bound forms of the metabolically important, intrinsically fluorescent biomolecule NADH (reduced nicotinamide adenine dinucleotide) [27, 28]. By exciting the sample with two pulse shapes in succession, we are able to rapidly determine enzyme binding of NADH without needing to measure the fluorescence spectrum or absolute yield. As discussed in more detail below, the approach is ideal for multiphoton microscopy with molecular discrimination and should be generally applicable to any fluorescent biological or chemical molecule that can be two- or three-photon excited by near-infrared light.

2. Experimental approach

We use laser pulses from an amplified Titanium Sapphire laser system that produces approximately 30 fs pulses at 1 kHz repetition rate centered at 780 nm. The pulses are shaped in an acousto-optic modulator based pulse shaper [5], split with a $50/50$ beamsplitter, and directed into either one or two cuvettes. Most of the measurements were carried out with focal intensities on the order of 1×10^{11} W/cm^2, although measurements at lower intensities showed identical results. The cuvettes contain solutions of either NADH alone in Trizma buffer, or NADH plus an enzyme in 3.2 M ammonium sulfate solution and Trizma buffer. We measure fluorescence from the two-photon excited molecules with two photomultiplier tubes (PMTs) by collecting light from the cuvettes at 90 degrees with respect to the laser propagation axis. Schott BG39 filters and high-reflecting dielectric mirrors at 780 nm are placed in front of the PMTs to eliminate

#155285 - $15.00 USD Received 26 Sep 2011; revised 13 Oct 2011; accepted 15 Oct 2011; published 16 Nov 2011
(C) 2011 OSA

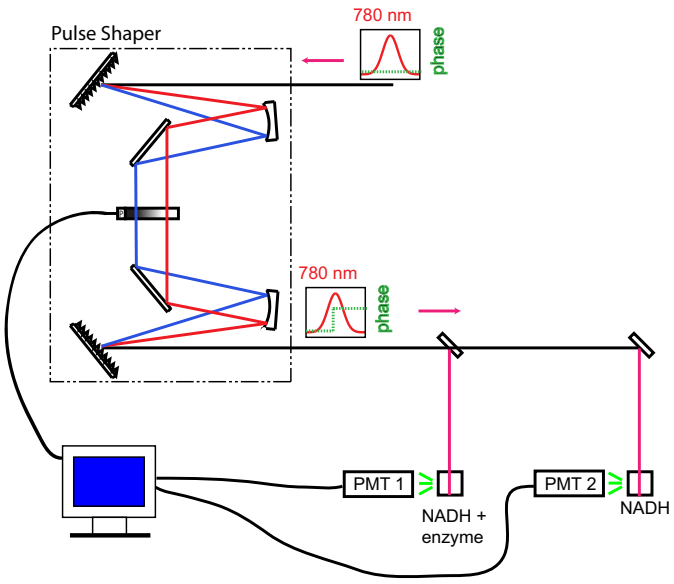

Fig. 1. Experimental set-up showing the computer-controlled pulse shaper and cuvettes containing NADH or NADH + enzyme in solution. As discussed in the text, the pulse shaper scans the position of a π-spectral phase step across the bandwidth of the laser pulse.

Rayleigh scattering from the excitation laser. The experimental apparatus is shown schematically in Fig. 1.

The single-photon spectral characteristics of NADH relevant to the experiment are shown in Fig. 2. The left panel plots the one-photon absorption spectrum of NADH alone, as well as NADH bound to the enzyme malate dehydrogenase (MDH); upon binding to MDH, the absorbance both increases and shifts slightly to the red, from 340 nm to 348 nm. The right panel shows the one-photon *fluorescence* spectrum for both unbound and enzyme-bound NADH; upon binding to MDH, the emission both strengthens and shifts slightly to the blue, nearing 450 nm center wavelength after one-photon excitation at 385 nm. The two-photon absorption profile of NADH has also been measured, and it shows a strong peak that extends from below 700 nm to 800 nm [27, 29]. After two-photon excitation it fluoresces over a broad ($\sim$ 30 nm) band centered near 460 nm (although not required, tuning the laser further to the blue would produce a substantial increase in signal).

Our goal is to discriminate between samples containing either unbound or enzyme-bound NADH using shaped pulses, and the particular pulse shapes we use for discrimination involve a spectral phase step of π radians at a given location within the bandwidth of the excitation pulse, leaving the spectral amplitudes unchanged (see inset of Fig. 1). Specifically, we monitor fluorescence from both pure NADH and NADH-plus-enzyme as the position of the π-phase step is scanned across the laser bandwidth. This parametrization is motivated by applications in atomic physics, where a π change in the spectral phase near a two-photon resonance keeps all frequency components contributing constructively to the transition probability [30]; similar schemes have been used for both higher-order perturbative transitions as well as strong-field effects (see for example [31, 32]).

To see the effect of a π-phase step on the pulse, Fig. 3 shows second-harmonic generation,

#155285 - $15.00 USD Received 26 Sep 2011; revised 13 Oct 2011; accepted 15 Oct 2011; published 16 Nov 2011
(C) 2011 OSA

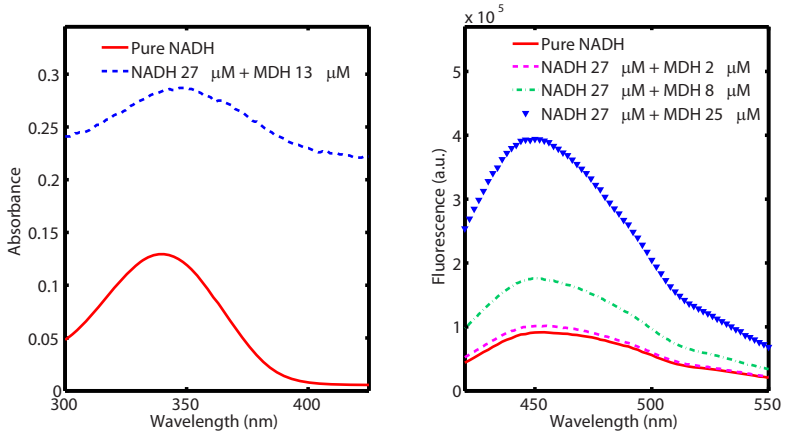

Fig. 2. Left panel: one-photon absorption spectrum of NADH and NADH plus MDH. Right panel: one-photon fluorescence spectrum of NADH and NADH plus MDH at various concentrations as measured in a spectrofluorometer. The excitation wavelength was 385 nm.

frequency-resolved optical gating (SHG-FROG) plots [33] for both an unshaped pulse (left panel) and for a pulse with a π-phase step located in the center of the spectrum (middle panel). The right panel shows the second-order power spectrum for pulses with a π-phase step at two different locations corresponding to the data shown in Fig. 4. More discussion of this panel is given below.

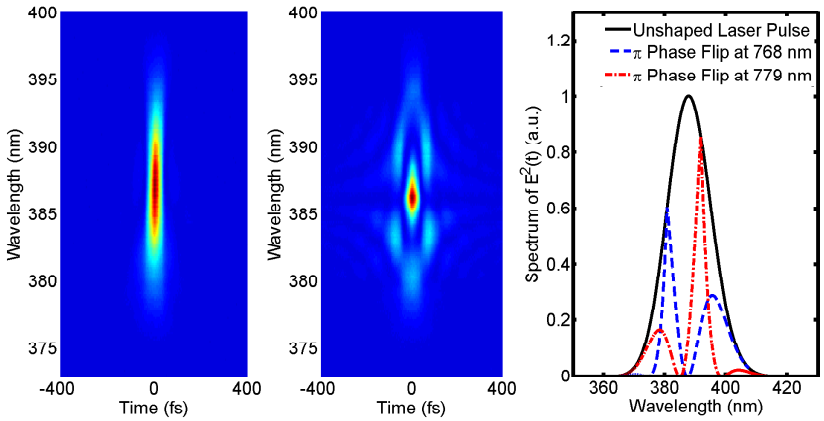

Fig. 3. SHG-FROG plots showing both an unshaped pulse (left panel) and a shaped pulse with a π-phase step in the middle of the spectral bandwidth (middle panel). The right panel shows the second-order power spectrum, or the Fourier transform of the square of the electric field in time, for an unshaped pulse and two π-phase step pulses that are representative of the control pulses used in Fig. 4.

In the limit of a narrow, two-photon atomic transition, such a scan produces a broad decrease in the fluorescence as the phase step scans across the laser bandwidth. However when the step is positioned at the two-photon resonance, spectral components both above and below the transition frequency contribute constructively, and the fluorescence once again increases to

#155285 - $15.00 USD Received 26 Sep 2011; revised 13 Oct 2011; accepted 15 Oct 2011; published 16 Nov 2011
(C) 2011 OSA

that of an unshaped pulse. This result can also be understood by considering the second-order power spectrum of the pulse, or the Fourier transform of the *square* of the electric field in time: $\mathscr{F}\left(E^2(t)\right)$. In the perturbative limit, the second-order power spectrum can be compared to the two-photon absorption spectrum to determine the excitation probability. A π-phase step has the property of producing a narrow spike in the two-photon spectrum at the position of the step (see Fig. 3 right panel) [34]. When the π-phase step is at the position of the resonance, the spectral density of the two-photon power spectrum at the position of the step is the same as for an unshaped pulse, thereby producing equivalent fluorescence.

In the inhomogeneously-broadened limit that often arises for large molecules in solution (where the molecular absorption line is much wider than the laser bandwidth), the central coherent spike at the resonance is suppressed and the scan resembles a relatively featureless single dip in the fluorescence [30]. We find that data from NADH in both its unbound and enzyme-bound forms appears to lie somewhere between these two extreme cases, and slightly different response curves between the two forms imply that a ratio of the signals can easily distinguish between them.

3. Results and discussion

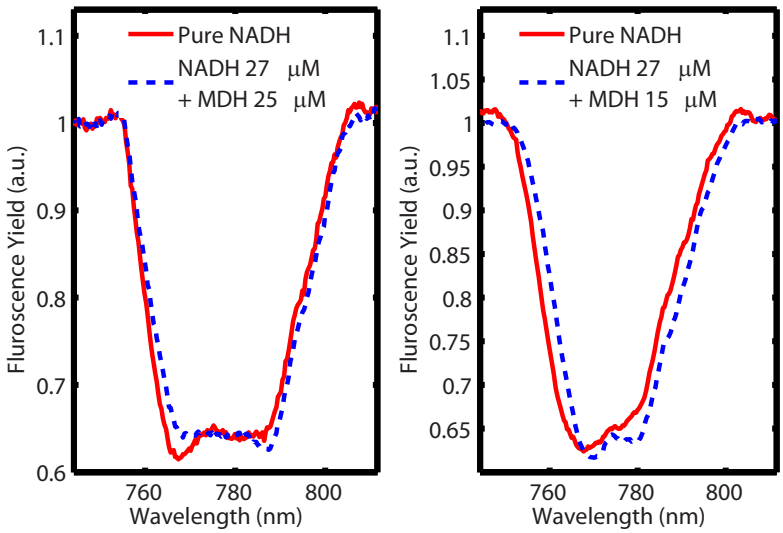

Fig. 4. Normalized fluorescence as a function of π-step position for both NADH alone (solid red) and NADH with MDH (dashed blue). The fluorescence from the Trizma buffer and MDH alone were negligible and did not affect the control. Measurements from two separate days are shown in the left and right panels to illustrate the fact that while the details of the scans vary from day to day, the main discrimination feature remains.

The normalized fluorescence as a function of π-phase step position for two different molecular solutions are shown in Fig. 4 (left and right panels show results from two separate days). The primary features the control exploits are the existence of the "double-minima" in the curves for both unbound (solid red curve) and enzyme-bound (dashed blue curve) NADH and the change in relative depth of the two minima with enzyme binding. In the left panel, the dip positions are at 767 and 787 nm (laser spectrum centered at 778 nm), while in the right panel the positions are 768 and 779 nm (laser spectrum at 775 nm). To see how the ratio of the two minima enables

#155285 - $15.00 USD Received 26 Sep 2011; revised 13 Oct 2011; accepted 15 Oct 2011; published 16 Nov 2011
(C) 2011 OSA

discrimination between the enzyme-bound and unbound molecules, Fig. 5 plots the *ratio* of the signals at the two minima in the curves as the MDH concentration is increased. An estimate of the binding fraction is shown across the top of the graph. These numbers are based on a measured dissociation constant of 4.7 μM [35] in the equilibrium formula $K_d = \frac{[N]\times[M]}{[A]}$, where $[N]$, $[M]$, and $[A]$ are the equilibrium molar concentrations of NADH, MDH, and NADH bound to MDH, respectively. The net result is that we find the short-wavelength minimum becomes less pronounced as the enzyme concentration increases.

Although the detailed structure of the curves shown in Fig. 4 was sensitive to pulse chirp and the shape of the laser spectrum, the monotonic increase in this ratio was consistent over several separate measurements. As an aside, since we are imaging fluorescence from a thick sample (path length 10 mm), the pulse undergoes moderate dispersion within the sample and a perfectly transform-limited pulse is not preserved. This would not be the case in a microscopic environment with 3D excitation, and we expect the detailed structure of the curves to be less sensitive to pulse chirp. Either way, the control was unaffected by these day-to-day changes. This monotonic behavior allows one to exploit the fluorescence ratio from two different pulse

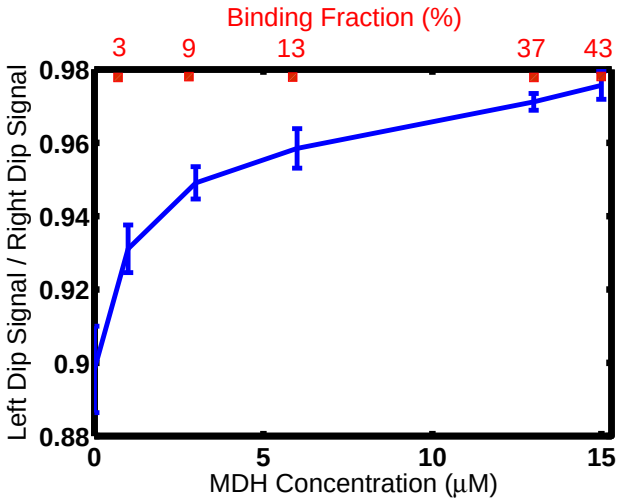

Fig. 5. Ratio of the fluorescence signal at the short-wavelength minimum to that at the long-wavelength minimum as a function of enzyme concentration. The binding fraction (as calculated based on the K_d value given in [35]) is shown on the top of the graph. The error bars show the standard deviation of the mean for repeated measurements.

shapes to determine the extent of enzyme binding in the laser focus. A natural choice for this experiment would be the pulse shapes located at each of the two minima in the π-phase scan; as can be seen in Fig. 5, the pulse shape producing the short-wavelength minimum ("left dip") selectively excites the enzyme-bound form as compared to the pulse shape producing the long-wavelength minima ("right dip").

While a complete understanding of the mechanism is not required to utilize the control in a microscopy environment, we consider one possible mechanism for the discrimination. Given the discussion above, the two-photon power spectrum of the pulse is a natural starting point. As as example, the right panel in Fig. 3 shows the two-photon power spectrum for a representative pulse with no spectral phase, as well as two shaped pulses with π-spectral phase steps at the two positions suggested in Fig. 4 (768 and 779 nm). Moving the step position to the blue or red changes where the spectral density in the second-order spectrum lies, suggesting that tuning the

#155285 - $15.00 USD Received 26 Sep 2011; revised 13 Oct 2011; accepted 15 Oct 2011; published 16 Nov 2011
(C) 2011 OSA

second-order spectrum could explain the observed control. In order to determine whether the two-photon power spectrum of our pulses is driving the discrimination, we need to know the two-photon absorption spectrum of both NADH and MDH-bound NADH. Although these have been measured [36], the resolution and signal-to-noise levels in available data are insufficient to either confirm or exclude this as a possible control mechanism. We note that a π-phase step is another example of quantum-control spectroscopy, where phase shaping in a spectrally-resolved, Fourier-based shaper is used to tailor the non-linear spectrum of a pulse. It may be that approaches like this can serve as complementary methods for measuring such quantities as two-photon absorption profiles.

An alternative way of highlighting selectivity between unbound and enzyme-bound forms in the face of laser or other noise is to examine histograms for the ratio of fluorescence for two different pulse shapes. Figure 6 shows histograms for measurements with NADH alone (pink shaded) and NADH with MDH (solid blue) using pulse shapes that were chosen for discrimination based on Fig. 4 (π-phase steps at 768 nm and 779 nm). Each histogram shows the number of measurements recorded that resulted in a given *ratio* of fluorescence for the two pulse shapes. Although the values of the actual dip ratios may change day-to-day, we find that for a given laser spectrum the ratios depend only on the enzyme concentration.

The histograms are separated by many standard deviations, illustrating that the two pulse shapes permit easy discrimination between the different forms of NADH even in the face of laser and sample fluctuations. This should be particularly useful in the broader research area of discrimination-based microscopy. Specifically, our results show promise for microscopy experiments where changes in molecular function or transformation (e.g. enzyme binding) need to be monitored in real time. Rapidly switching between pulse shapes with software modifications allows one to discriminate between molecular subspecies on a near shot-by-shot basis. Although the degree of control in a given trial may be modest, the experiment readily achieves the essential feature of control exceeding the noise that is required for discrimination. For example, as Fig. 5 illustrates, we are sensitive to binding fractions as low as 3%, with the sensitivity largely limited by the amount of signal averaging that one is able to perform. This selectivity enables one to create high-contrast fluorescent images of samples containing multiple fluorophores. We expect this approach to be very general, and in cases where simple pulse shape parameterizations such as the one above are insufficient, a feedback approach [7] should allow for even wider applicability. Finally we note that the observed control is not sensitive to the energy of the input pulse. As long as the intensity is sufficient to observe two-photon fluorescence, pulse shapes chosen from the two minima produced selective excitation of either the unbound or enzyme-bound form.

4. Conclusion

In conclusion, we have shown how pulse shaping in conjunction with multiphoton absorption can be used to distinguish between unbound and enzyme-bound biomolecules in solution. The control exploits different responses between the two forms to spectral phase shaping, and the results are promising for the prospect of discrimination based microscopy. We gratefully acknowledge support from the National Science Foundation under Grant No. 0854922 and Dickinson College. We also thank Suzanne Scarlatta, Mark Bowen, and Alexander Orlov at Stony Brook University for the generous use of a spectrofluorometer and a spectrophotometer.

5. Appendix: materials and methods

NADH: Acros, CAS 606 – 68 – 8
MDH: Roche, Suspension in 3.2 M ammonium sulfate solution, pH approx. 6,
Trizma: Sigma Aldrich, hydrochloride buffer solution, pH 7.0, 1 M

#155285 - $15.00 USD Received 26 Sep 2011; revised 13 Oct 2011; accepted 15 Oct 2011; published 16 Nov 2011
(C) 2011 OSA

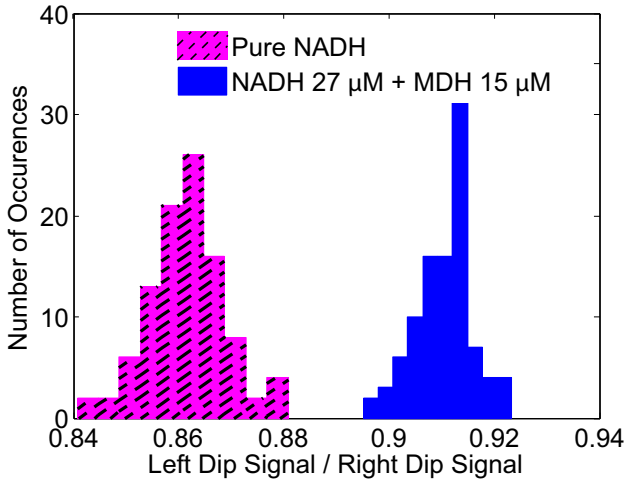

Fig. 6. Histograms showing the ratio of fluorescence between two pulse shapes for both unbound NADH (pink shaded) and enzyme-bound NADH (solid blue). The clear distinction between the peaks implies easy selectivity between the two forms of NADH. The peaks were constructed from 100 measurements, with 500 laser shots contributing to each measurement.

Powdered NADH was first mixed into Trizma solution to reach the desired molar concentration. MDH in 3.2 M ammonium sulfate solution was then mixed into the buffered NADH solution to reach the stated molar concentrations. Although the fraction of NADH that is enzyme bound in a particular mixture is a function of the respective molar concentrations, for simplicity we refer to the solution containing both NADH and MDH as “bound” NADH. For typical data shown in the paper, we expect the sample to have an actual binding fraction of approximately 40%.

#155285 - $15.00 USD Received 26 Sep 2011; revised 13 Oct 2011; accepted 15 Oct 2011; published 16 Nov 2011
(C) 2011 OSA